Simulation study on correction of titanium alloy adaptive deformable mirror based on random phase method

Xiaoqin Yan[*a,b,c], Zibo Jiang[a,b]
[a]Nanjing Institute of Astronomical Optics & Technology, Chinese Academy of Sciences, Nanjing 210042, China; [b]CAS Key Laboratory of Astronomical Optics & Technology, Nanjing Institute of Astronomical Optics & Technology, Nanjing 210042, China; [c]University of Chinese Academy of Sciences, Beijing 100049, China

ABSTRACT

This paper focuses on the phase distortion problem caused by atmospheric turbulence and conducts research based on titanium alloy metal adaptive ultra-thin mirrors by using numerical simulation and modeling methods. Specifically, the Zernike polynomial method was adopted to simulate the distorted wavefront of atmospheric turbulence, and the simulation results were verified. Based on the finite element analysis results of the metal ultra-thin mirror, the influence function of a single actuator was fitted using the super-Gaussian function. The correlation coefficient for the matching degree of the obtained influence function exceeded 0.9. Then, the distorted wavefront was corrected by the fitted influence function. After correction, the root means square value (RMS) of the distorted wavefront decreased by 77.56%, which verified the feasibility of correcting wavefront distortion with titanium alloy metal mirrors.

Keywords: Deformable mirror, titanium alloy, adaptive mirror, atmospheric turbulence, phase screen, influence function

1. INTRODUCTION

Atmospheric turbulence is a complex natural phenomenon that has a significant impact on the propagation of light waves in the atmosphere, and the phase distortion problem is particularly prominent. In numerous optical application fields, such as astronomical observation and free-space optical communication, phase distortion caused by atmospheric turbulence severely restricts the performance and accuracy of the system[1,2]. In 2019, Jiang, Z. B., et al. conducted a study on the influence of indoor air turbulence on imaging quality. The research results indicated that with the increase of disturbance intensity or turbulence intensity, optical quality would decline to a certain extent[3]. To address this challenge, adaptive optics technology emerged. In adaptive optics systems, ultra-thin mirrors used to correct distorted wavefronts are of vital importance. Compared with traditional glass ultra-thin mirrors, metal ultra-thin mirrors have obvious advantages. On the one hand, their characteristic of being less prone to breakage effectively reduces the risk of damage and development costs. On the other hand, they possess excellent thermal conductivity, high tensile strength, and a low coefficient of thermal expansion, which can effectively suppress temperature deformation.

To verify the performance of metal ultra-thin mirrors, it is necessary to generate random phases representing the distortion caused by atmospheric turbulence and correct them. In 2005, Zhang, H. M., et al. simulated the wavefront distorted by atmospheric turbulence using the power spectrum inversion method and the Zernike polynomial method and verified the fitting results[4,5]. In 2018, Luo, S., et al. conducted studies on the correction ability of piezoelectric ceramic actuators based on the influence function of deformable mirrors[6].

This paper proposes a systematic approach to researching atmospheric turbulence distortion by comprehensively applying numerical simulation and modeling methods using titanium alloy adaptive deformable mirrors. Firstly, the Zernike polynomial method is adopted to simulate atmospheric turbulence distortion. Then, based on the finite element analysis (FEA) results of ultra-thin mirrors, the influence function model of a single actuator is fitted. We correct the distorted wavefront using the influence function obtained through fitting. Through this series of studies, the aim is to verify the effectiveness of this method in wavefront correction.

[*]xqyan2023@niaot.ac.cn

International Conference on Optics, Electronics, and Communication Engineering (OECE 2025), edited by Yang Yue, Proc. of SPIE Vol. 13965, 139654J
 · 0277-786X · doi: 10.1117/12.3089777

2. SIMULATION OF ATMOSPHERIC TURBULENCE DISTORTION PHASE SCREEN

Research on wavefront correction for atmospheric turbulence is of great significance for improving the imaging quality of optical systems. At present, there are mainly three methods for studying the wavefront distortion problem caused by atmospheric turbulence: experimental analysis, theoretical model analysis and numerical simulation. The first two have certain limitations and thus are restricted in application, while numerical simulation can construct an atmospheric turbulence phase screen, conveniently and effectively studying transient atmospheric turbulence, with obvious advantages. The existing numerical simulation methods for obtaining the phase screen of atmospheric turbulence distortion can be classified into three categories: power spectrum inversion method[7], Zernike mode expansion method[8], and fractal method[9-11].

Based on the covariance expression of the Zernike polynomial derived from Noll[12], Roddier, N. proposed an algorithm for simulating the distorted wavefront of the atmosphere in 1990. The core of this algorithm is to perform Zernike expansion using the randomly weighted Karhunen-Loeve function. Based on this algorithm, the wavefront distortion phase screen under Kolmogorov turbulence was simulated in MATLAB, where the wavelength was 632.8nm, the coherence length r_0=0.1m, the resolution size of the generated phase screen was 256×256, and the aperture was 0.15m.

Figure 1 shows the atmospheric turbulence distortion phase screen generated when the Zernike polynomial is 30 terms. It can be clearly seen from Figures 1 and 2 that the generated phase screen is mainly composed of low-frequency components, and the most severe distortion is the tilt component.

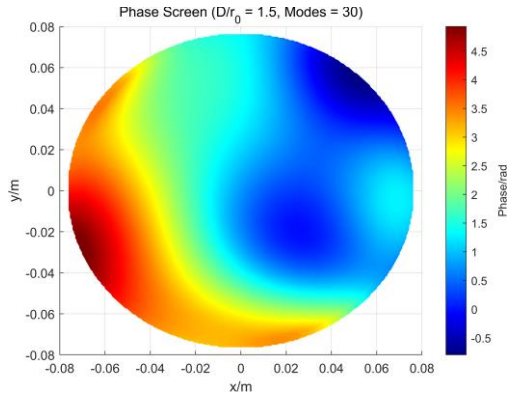

Figure 1. Schematic diagram of the atmospheric turbulence distortion phase screen.

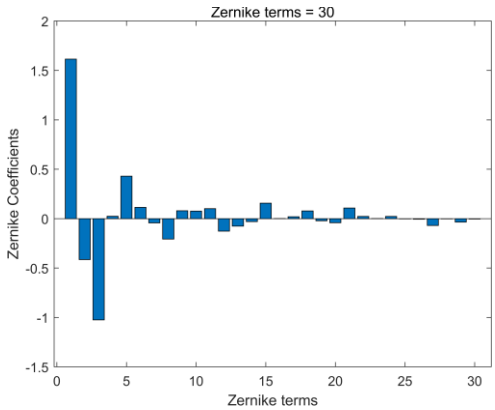

Figure 2. The coefficients of 30 terms corresponding to the atmospheric turbulence distortion phase screen.

3. FINITE ELEMENT SIMULATION AND INFLUENCE FUNCTION FITTING OF TITANIUM ALLOY ULTRA-THIN MIRROR

In this section, the finite element simulation and numerical fitting of the influence function of the titanium alloy ultra-thin deformable mirror supported by 19 voice coil actuators under its own gravity deformation are studied. After achieving the numerical fitting of the influence function of deformable mirror, the magnitudes of the forces required to correct the atmospheric turbulence distortion phase can be calculated, thus enabling the real-time correction of the atmospheric turbulence distortion screen.

3.1 Simulation of gravity deformation of titanium alloy ultra-thin deformable mirror

Titanium alloy is chosen as the material for the ultra-thin adaptive secondary mirror due to its unique physical properties that differ from glass. It is not as brittle as glass, reducing the risk of damage and the cost of development, and increasing the safety factor. It also has high thermal conductivity, high tensile strength, and a low coefficient of thermal expansion, which can reduce the effect of temperature-induced deformation.

The support base of the ultra-thin mirror employs fixed support constraints. The density of the titanium alloy ultra-thin mirror is 4.51×10^3 kg/m³; the Young's modulus is 110 GPa; the specific stiffness is 24.39 MPa·m³/kg; the Poisson's ratio is 0.34. The thickness of the ultra-thin mirror affects the correction force and gravity deformation. The thinner the mirror, the smaller the correction force required, but the gravity deformation increases as the thickness decreases. Therefore, an

appropriate thickness needs to be selected to balance the two. The diameter of this ultra-thin mirror is 0.15 m, and it adopts a layout of one actuator in the middle, six actuators on the second circle, and twelve actuators on the third circle, with a spacing of 33 mm between each circle, as shown in Figure 3.

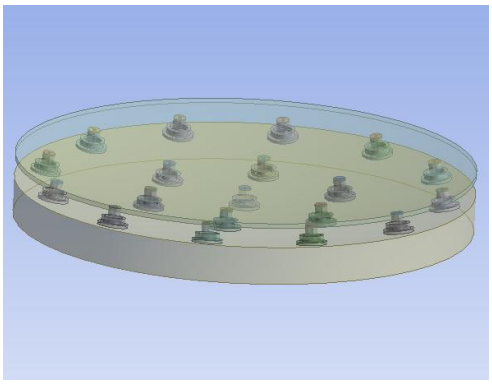

Figure 3. A titanium alloy ultra-thin mirror supported by 19 voice coil motors.

Finite element analysis of gravity-induced deformation was carried out on the ultra-thin mirror with thicknesses of 0.8 mm, 1 mm, 1.2 mm, and 1.5 mm, and the results are presented in Figure 4. The gravity-induced deformation displacements of the mirror surface at different thicknesses can also be obtained, as shown in Table 1. Combining Figure 4 and Table 1, it can be seen that the gravity-induced deformation of the ultra-thin mirror increases as the thickness decreases. Due to the limited number of actuators, the edge of the mirror is more affected by gravity as the thickness decreases, affecting the RMS value of the mirror surface shape. A comprehensive analysis indicates that when the thickness is 1.2 mm, the PV value is close to λ/30, meeting the usage requirements of this study.

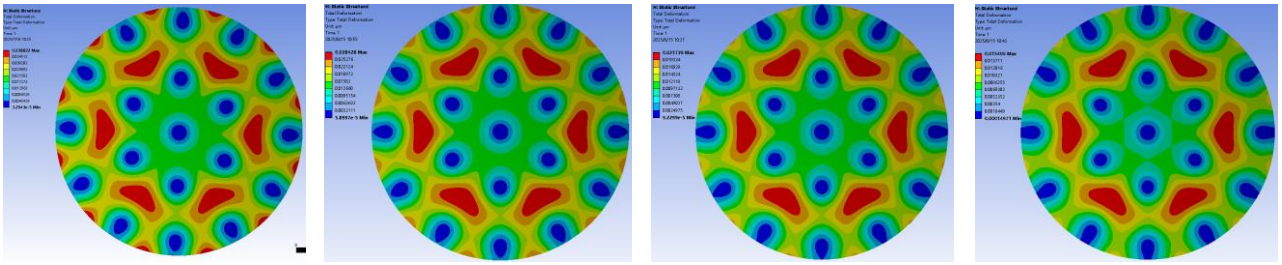

(a) the case with thickness 0.8mm (b) the case with thickness 1mm (c) the case with thickness 1.2mm(d) the case with thickness 1.5mm

Figure 4. The results of gravitational deformation under different mirror thicknesses.

Table 1. Gravitational deformation displacement of mirrors at different thicknesses.

Thickness/mm	RMS/nm	PV/nm
0.8	9.7961	38.789
1	7.1221	28.369
1.2	5.3832	21.647
1.5	3.7894	15.256

3.2 Numerical fitting of the influence function of the ultra-thin mirror

The influence function of the adaptive deformable mirror can be represented by a super-Gaussian function $f_i(x, y)$, which is usually determined by the actuators spacing, actuators layout, boundary constraint conditions, and material elastic modulus.

$$f_i(x,y) = \exp[\ln \omega(\sqrt{(x-x_i)^2 + (y-y_i)^2}/d)^{\alpha}] \quad (1)$$

In the formula, $f_i(x, y)$ represents the influence function of the i-th actuator, d is the actuator spacing, α is the Gaussian exponent, and ω is the actuator crosslinking value, which is the ratio of the deformation α_1 of the actuator that is energized in a single influence function to the deformation α_2 of the adjacent actuator, $\omega = \alpha_1/\alpha_2$, ranging from 5% to 20%. A larger crosslinking value indicates a greater influence between adjacent actuators, and different crosslinking values can significantly affect the wavefront correction capability of the deformable mirror.

Finite element simulation was conducted by ANSYS on the influence function of a single actuator. Due to the symmetry of the model, only one actuator in each circle was simulated. During the simulation, a force with 1N was applied to the actuator, while no force was applied to the others. Fixed support constraints were applied to the edge of the ultra-thin mirror. At this time, the mirror surface shape of the deformable mirror was the influence function of the actuator. Figure 5 shows the cloud maps of the influence functions of actuators in different circles. The influence function of the central actuator is close to the ideal super-Gaussian function, and the deviation becomes more severe as it approaches the edge, which is due to the edge effect.

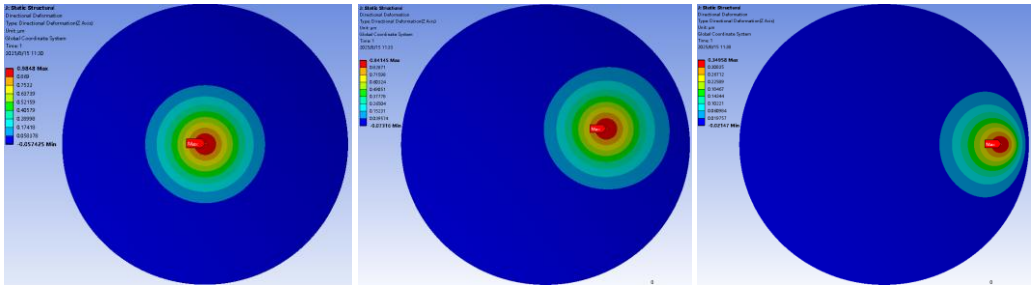

Figure 5. The influence functions of each actuator obtained through ANSYS simulation.

To effectively correct the distorted wavefront caused by atmospheric turbulence, it is necessary to obtain an accurate mathematical characterization of the influence function of a single actuator. This function is usually fitted and modeled using a super-Gaussian function (formula 1). The obtained surface shape data was imported into MATLAB and an initial parameter was set to fit the influence function. The fitting results are shown in Figures 6 and 7. Figure 6 describes the three-dimensional fitting result of the central actuator. The fitted model is in good agreement with the simulation results, verifying the correctness of the super-Gaussian function as the mathematical model for fitting the influence function.

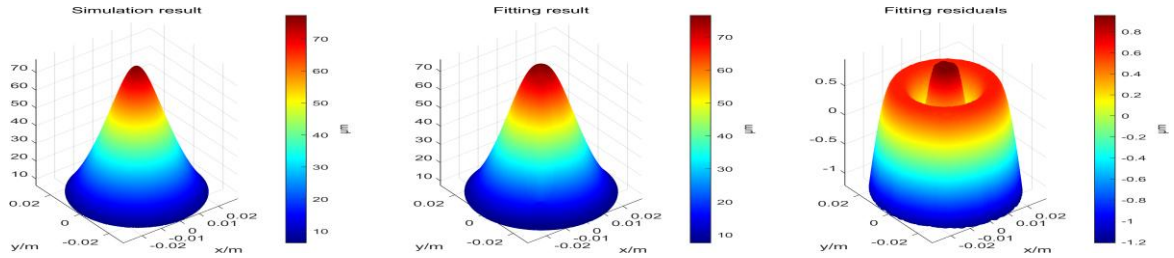

(a) Simulation result (b) Fitting result (c) Fitting residuals

Figure 6. Comparison of the simulation results and fitting results of the central actuator.

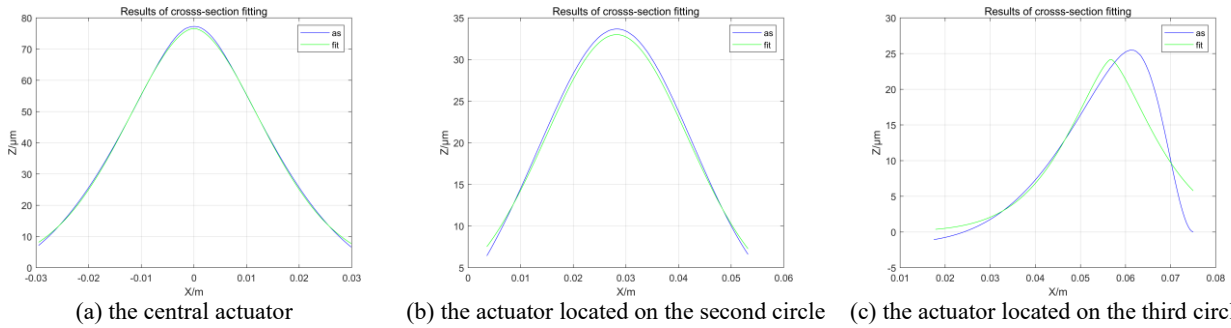

(a) the central actuator (b) the actuator located on the second circle (c) the actuator located on the third circle

Figure 7. The profile fitting results of the three actuator influence functions.

Table 2 presents the super-Gaussian function fitting parameters for three actuators. The correlation coefficient R^2 ($0 \leq R^2 \leq 1$) represents the matching degree of the fit, and the closer it is to 1, the better the fitting effect. The data in Figure 7 and Table 2 also verify the simulation results: the influence function of the central actuator is close to the ideal super-Gaussian function, and the correlation coefficient of the fitted influence function of the outermost circle actuator drops to 0.9306, indicating a slightly poorer fitting effect.

Table 2. Three actuator influence function fitting parameters.

Actuator	ω	α	R^2
Central	0.06491	1.7870	0.9993
The second circle	0.06219	1.7347	0.9990
The third circle	0.03675	1.4125	0.9306

4. CORRECTION OF WAVEFRONT DISTORTION OF LIGHT

Suppose the required mirror surface deformation to correct the wavefront distortion is $W(x, y)$, the influence function of the i-th actuator is $f_i(x, y)$, and the force F_i that the i-th actuator needs to apply to correct the wavefront distortion is given. Let there be N actuators in total. To correct the distorted wavefront, the correction forces applied by each actuator should satisfy:

$$W(x,y) = \sum_{i=1}^{N} f_i(x,y) \cdot F_i \tag{2}$$

That is,

$$W_{M\times 1} = f_{M\times N} \cdot F_{N\times 1} \tag{3}$$

The approximate solution obtained by the least squares method is:

$$F = (f^T \cdot f)^{-1} \cdot f^T \cdot W \tag{4}$$

To more intuitively observe the effect of correcting the distorted wavefront using the fitted influence function, a distorted wavefront caused by atmospheric turbulence with 100 terms of Zernike polynomials was generated through numerical simulation, and the forces of the 19 actuators required for correction were calculated using the fitted influence function, as shown in Table 3.

Table 3. The force required to correct the 19 actuators of the distorted wavefront.

Actuator	Force/N	Actuator	Force/N	Actuator	Force/N
1	-0.0799	8	-0.2281	15	-0.1201
2	-0.0895	9	-0.4142	16	0.0572
3	-0.1355	10	-0.6327	17	0.2776
4	-0.1404	11	-0.3286	18	0.0858
5	-0.1030	12	-0.4654	19	-0.2997
6	0.0026	13	-0.2909		
7	-0.0163	14	-0.2994		

The corrected wavefront is also shown in Figure 8b. The RMS value of the surface shape before correction was 167.207 nm, and the peak-to-valley (PV) value was 516.344 nm. After correction, the RMS value of the surface shape reached 37.528 nm, and the PV value reached 308.388 nm. From the RMS values before and after correction, the correction efficiency reached 77.56%. Therefore, it can be concluded that the titanium alloy ultra-thin deformable mirror supported

by 19 actuators has a good ability to correct distorted wavefronts. If the number of actuators is appropriately increased and they are reasonably arranged, a better correction effect can be achieved.

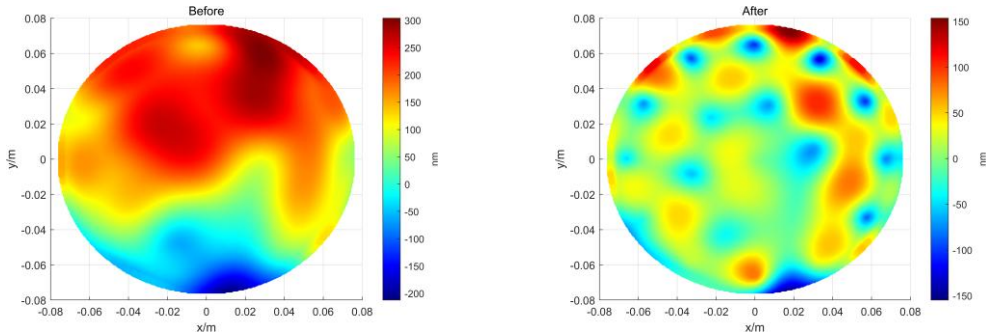

(a) Distorted wavefronts obtained from simulation (100 terms) (b) The wavefront after correction

Figure 8. The wavefront before and after correction.

5. CONCLUSION

This paper has conducted a series of studies on the phase distortion caused by atmospheric turbulence. The self-gravity deformation of a titanium alloy ultra-thin deformable mirror with a diameter of 150 mm supported by 19 actuators was analyzed, and the thinning thickness of the ultra-thin mirror was determined. On this basis, a systematic study on the influence function of the actuator s was carried out. The function model of a single actuator was fitted using a super-Gaussian function based on finite element analysis. The fitted function model can well describe the influence function of a single actuator, and the correlation coefficients all reached above 0.9. Using the super-Gaussian function to replace the actual influence function can be used to calculate the forces of the actuators required to correct the distorted wavefront. Through calculation, it was found that after correcting the RMS of the generated distorted wavefront was 37.528 nm, which was reduced by 77.56%.

ACKNOWLEDGMENT

This paper is supported by the following project, and we would like to express our gratitude: 1. Key research and development project: “Frontier Technology Research on Large Astronomical Optical Infrared Telescope”, project number: 2022YFA1603000.2. National Natural Science Foundation of China (General Program): the research of the key technologies on fabrication and testing of large diameter and ultra-thin convex hyperbolic mirror. Project Approval Number:11673044. 3.Technical Innovation Project of Instrument and Equipment Function Development of the Chinese Academy of Sciences: “Development of Discrete Symmetric Loading Device for Stressed Mirror Annular Polishing”.

REFERENCES

[1] Yang, Q., Zhu, J. P. and Cao, G. R., “Optimal Design of dual piezoelectric Deformable Reflectors,” Acta Optica Sinica 19(5), 613-618 (1999).
[2] Liu, J., Wang, P. and Zhang, X., “Deep learning based atmospheric turbulence compensation for orbital angular momentum beam distortion and communication,” Optics Express 27(12), 16863-16873 (2019).
[3] Jiang, Z. B., Chen, Z. and Kou, S. F., “Research on the influence of air turbulence of vertical long optical path on wave front detection,” AOPC 2019 113410G-1-113410G-10 (2019).
[4] Zhang, H. M. and Li, X. Y., “Research on Numerical Simulation Method of Atmospheric Turbulence Distortion Phase Screen,” Opto-Electronic Engineering (01), 14-19 (2006).
[5] Zhang, H. M., [Preliminary Study on Numerical Simulation of Turbulence Effects in Laser Atmospheric Transmission], Sichuan: Institute of Optics and Electronics, Chinese Academy of Sciences, Doctor’s Thesis, (2005).

[6] Luo, S., Wang, J. Q. and Zhang, B., “The influence of fatigue characteristics of piezoelectric ceramic actuators on the correction ability of deformable mirrors,” Chinese Journal of Lasers 45(09), 289-294 (2018).
[7] McGlamery, B. L., “Restoration of turbulence-degraded images,” Journal of the Optical Society of America 57, 93-297 (1967).
[8] Roddier, N., “Atmospheric wavefront simulation using Zernike polynomials,” Optical Engineering 29(10), 1174-1180 (1990).
[9] Lane, R. G., Glindemann, A. and Dainty, J. C., “Simulation of a kolmogorov phase screen,” Waves in Random Media 2(3), 209-224 (1992).
[10] Schwartz, C., Baum, G. and Ribak, E. N., “Turbulence degraded wave fronts as fractal surfaces,” Journal of the Optical Society of America 11, 444-451 (1994).
[11] Wu, H. L., Yan, H. X., Li, X. Y., et al., “A rectangular turbulent phase screen is generated based on the fractal characteristics of the distorted phase wavefront,” Acta Optica Sinica 29(1), 114-119 (2009).
[12] Noll, R. J., “Zernike polynomials and atmospheric turbulence,” Journal of the Optical Society of America 66, 207-211 (1976).